A SIW-Fed Double-Helix Antenna With Broadband Circular Polarization for MMW Applications

Longye Li, Changhong Zhang, Yu Shao, Jiake Yin, and Jiangtao Luo, *Senior Member, IEEE*

***Abstract*—In this letter, a planar double-helix antenna with circular polarization is proposed for millimeter-wave (MMW) applications. The double helical strips are printed on the two opposite surfaces of the substrate in a 180° rotational symmetry and connected by metalized via-holes. The circularly polarized wave is achieved by the currents along strips and via-holes, which generate the horizontal and vertical polarization, respectively. In addition, currents along the ground edges near helixes are implemented to balance the amplitudes of electric fields along strips and via-holes for good circular polarization. To improve bandwidths and circular polarization performance, moderate tapered helixes are applied. With the advantages of low transmission loss, planar and fully enclosed structure, the substrate integrated waveguide is applied as the feeding line for easy integration with MMW circuitry. Experimental results show that the antenna obtains an operating bandwidth of 28.6% from 24 to 32 GHz, a peak gain of 7.8 dBic and a low profile of 0.14 λ_0 (λ_0 is free-space wavelength at the center frequency of 28 GHz).**

***Index Terms*—Broadband, circular polarization, double-helix, endfire radiation, substrate integrated waveguide.**

I. Introduction

With merits of mitigating multipath fading, avoiding "Faraday rotation", and alleviating polarization mismatch, circularly polarized (CP) antennas have been studied a lot over the past decades. Many methods have been proposed to design broadband CP antennas for high data-rate even up to gigabit-rank transmission in the developing fifth-generation (5G) systems operating in millimeter wave (MMW) bands. Due to low transmission loss, planar and fully enclosed structure, the substrate integrated waveguide (SIW) is very suitable as feeding lines for easy integration with planar circuits in MMW. Therefore, SIW-fed broadband CP antennas are much desired in the 5G MMW integrated systems.

Various kinds of CP antennas and arrays based on SIW in MMW bands had been designed and investigated, such as aperture antennas [1], [2], cavity antennas [3], [4], horn antenna [5], combined antenna [6], complementary source antennas [7], [8], and so on. In [1], a differentially-fed aperture antenna realized a high gain of 14.6 dBic by introducing four rectangular open loops over a large cavity, whereas the axial ratio bandwidth (ARBW) was 16.7%. In [3] and [4], by rotating rectangular patches above the slots, they could generate left-hand circular polarization (LHCP) or right-hand circular polarization (RHCP) radiation flexibly, but the available ARWBs were around 11.6% and 4.6%, respectively. In [5], a horn antenna realized a very low profile of 0.12 λ_0 by SIW technology. With a phase controlling and power dividing structure fully integrating inside the horn, the antenna realized CP radiation effectively, but its CP bandwidth was only 5.9%. In [6], by integrating the horn and Vivaldi antenna with a 90° hybrid, a CP combined antenna was designed. However, the antenna occupied a large space and suffered from a narrowed bandwidth of 9%. In [7], a CP complementary source antenna with a working bandwidth of 51% had been studied, but its peak gain was 6.4 dBic. For gain enhancement, a three-layer dielectric rod structure with extended length was applied and then a peak gain of 12.9 dBic was achieved, whereas it suffered from a profile of more than 0.50 λ_0. In summary, it appears challenging to design a CP antenna with a wide bandwidth, thin profile, and simple structure.

Compared with those antennas mentioned previously, the helical ones with the virtues in terms of endfire radiation, broad bandwidth, and outstanding circular polarization performance have been attracting more and more interests [9]. However, most of them suffered from the three-dimensional (3-D) structures with high profiles and bulky volumes such as [10] and [11], which deeply constrained their applications. Thus, lots of effects had been developed on compact helical antennas. Applying a low pitch angle and less turns of the helixes was a general way to cut down profile heights [12], [13], but they still could not avoid 3-D structure. In [14], a two-port planar differentially fed tapered helix antenna with parasitic units had been studied, but its ARBW was 20%. In [15], a planar helical antenna achieved a high CP gain of 11.5 dBic and a wide bandwidth of 31% with the aid of shaped dielectric lenses and plasma material. In [9], a very low helix antenna with height of 0.11 λ_0 was proposed. But both of them were fed by coaxial lines with asymmetric structures, which leaded to an asymmetric and deteriorated radiation pattern. Moreover, they were working in low frequency around 10 GHz. Low profile planar helix antennas [16] and [17] in MMW bands had been designed. But they were both linearly polarized antennas. Antennas mentioned above are usually bulky, costly, and hard to be integrated with other components and devices in the systems.

In this letter, a planar double-helix antenna with a low profile of 0.14 λ_0 in MMW band has been studied, which obtains the

Manuscript received October 28, 2021; revised November 26, 2021; accepted November 26, 2021. Date of publication December 1, 2021; date of current version February 3, 2022. This work was supported in part by the National Natural Science Foundation of China under Grant 61801070 and Grant 61701061; and in part by the Natural Science Foundation of Chongqing under Grant cstc2019jcyj-msxmX0606. *(Corresponding author: Changhong Zhang.)*

The authors are with the School of Communication and Information Engineering, Chongqing University of Posts and Telecommunications, Chongqing 400065, China (e-mail: s190101099@stu.cqupt.edu.cn; zhangch@cqupt.edu.cn; shaoyu@cqupt.edu.cn; 2018215030@stu.cqupt.edu.cn; luojt@cqupt.edu.cn).

Digital Object Identifier 10.1109/LAWP.2021.3131636

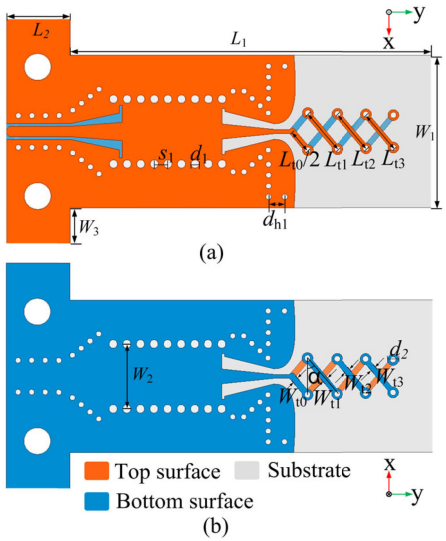

Fig. 1. Geometry of the proposed antenna. (a) Top view (top surface). (b) Bottom view (bottom surface).

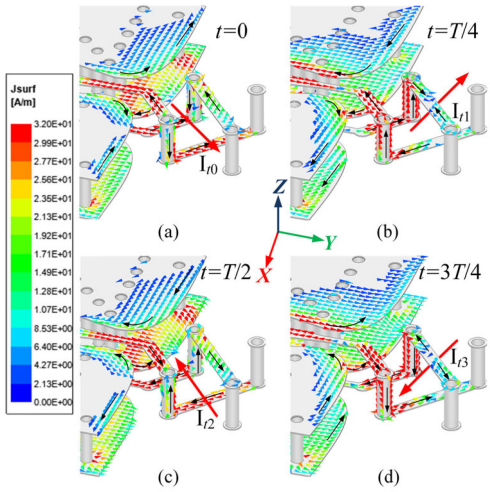

Fig. 2. Current distributions on the antenna over a period time at 27 GHz. (a) $t = 0$; (b) $t = T/4$; (c) $t = T/2$; (d) $t = 3T/4$.

wide impedance bandwidth (IBW) and ARBW of 29.3% and 30.4%, respectively, and a peak CP gain of 7.8 dBic. In summary, with simple, planar structure and wide available bandwidth, the antenna has great potential for 5G applications.

II. Antenna Design

A. Antenna Geometry and Working Principle

The configuration of the proposed antenna is plotted in Fig. 1. It owns three pairs of helical strips connected vertically by plated via-holes, as shown in Fig. 1(a). The strips are printed on both surfaces of the substrate in a 180° rotational symmetry. To improve bandwidths and AR performance, the lengths of strips are slightly tapered and the widths are narrowed by the ratios denoted by k and r individually according to the following ratios:

$$k = \frac{L_{t1}}{L_{t0}} = \frac{L_{t2}}{L_{t1}} = \frac{L_{t3}}{L_{t2}} \tag{1}$$

$$r = \frac{W_{t1}}{W_{t0}} = \frac{W_{t2}}{W_{t1}} = \frac{W_{t3}}{W_{t2}}. \tag{2}$$

Also, a pair of half-length strips is terminated with a parallel microstrip line for feeding, which also functions as the transition line between SIW and helixes. Compared to the coaxial-fed single helical antenna [15], the proposed double helical one will occupy less radiator space with the same number of helixes at the helix rotation angle unchanged. Generally, a large ground plane, which is vertical to the axis of helixes, is necessary in antenna designs. However, for the sake of low profile, a tapered ground with vertical side- and back-wall working as a replacement of reflector is utilized. It should be mentioned the currents on ground edges next to the helixes can weaken the stronger horizontal electric field, which promotes the CP radiation. Besides, additional grounded coplanar waveguide (GCPW) and SIW-to-GCPW transition are just applied for SMA connector for measurement. In this design, a Rogers 5880 substrate with a nonstandard thickness of 1.508 mm, a relative permittivity of 2.2, and a loss tangent of 0.0009 is applied.

There are several key design points. 1) For gain and bandwidth enhancement, the tapered helical strips are applied, which is verified in antennas [18]–[20]. The longer rods or strips function as the reflector for the shorter ones. A tapered ground is applied rather than stepped one [14] since a smooth physical structure tends to produce radiation pattern and input impedance that varies smoothly with frequency [18]. 2) To the best of the authors knowledge, almost all planar single-fed planar helix antennas are with single helix, but the proposed double-helix one will save radiator space and reduce antenna size with same number of turns at the turns' rotation angle unchanged. 3) Owning to SIW feeding, the antenna achieves a low profile height of 0.14 λ_0 and avoids extra room for coaxial line installation, which is extremely suitable to be integrated on surface applications such as missiles and aircrafts with PCB technology. Compared to coaxial-fed antennas [9], [15], the antenna also improves the degraded radiation patterns.

Fig. 2 shows the current distributions on the inner ground edges, the initial one and a half pairs of helical strips to illustrate the principle of CP radiation at 27 GHz. In Fig. 2(a), when $t = 0$, the currents along the connecting via-holes are both in $-z$-direction, which generate the vertically polarized radiation together. The currents along the strips on the same surface are in the same direction. So the angle of the currents between the upper and lower surface is 2α [α is the rotation angle of the helixes shown in Fig. 1(a)]. Consequently, the current in $-x$-direction is achieved, which generates the horizontally polarized radiation. It must be mentioned that the horizontal electric field magnitudes are weakened somehow by the currents along the ground edges, which also occurs at the time of $T/4$, $T/2$, and $3T/4$. It is beneficial for CP radiation since the fields on the horizontal fields are stronger than that of vertical ones. Due to the existence of the currents in $-z$ and $-x$-direction, a dominant current of I_{t0} is achieved. When $t = T/4$ shown in Fig. 2(b), the current distributions on the half-length strips are in accordance with those of $t = 0$, but the currents on via-holes are inverse.

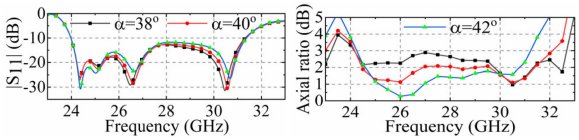

Fig. 3. Simulated performances of $|S_{11}|$ and AR versus α.

TABLE I
OPTIMAL PARAMETERS OF THE PROPOSED ANTENNA (UNIT: mm)

Parameter	W_1	W_2	W_3	L_1	L_2	L_{t0}	L_{t1}	L_{t2}	L_{t3}
Value	11	5	4.6	26	4.6	3.54	3.44	3.31	3.17
Parameter	W_{t0}	W_{t1}	W_{t2}	W_{t3}	d_1	d_2	d_{h1}	s_1	α
Value	0.44	0.41	0.39	0.37	0.4	0.6	1.47	1	40°

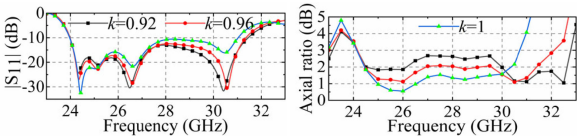

Fig. 4. Simulated performances of $|S_{11}|$ and AR versus k.

The currents on the other pair of strips are very weak. Therefore, the current of I_{t1} orthogonal to I_{t0} is achieved. In Fig. 2(c), the current distributions at $t = T/2$ are opposite to those at $t = 0$, which also generates the dominant but out of phase current I_{t2}. Similarly, I_{t3} is also out of phase to I_{t1} shown in Fig. 2(d). As a result, a RHCP endfire antenna has been carried out.

B. Parametric Study

Several vital parameters of the antenna including the rotation angle of the helixes α, the tapered length ratio k, the initial strip length L_{t0}, and the ground height d_{h1} have been studied, as shown in Figs. 3−6. When a parameter is discussed, others keep unchanged as tabulated in Table I.

Fig. 3 shows $|S_{11}|$ and AR performances with different tapered ratio α. With the increase of α from 38° to 42°, the curve of AR goes down gradually across 24.5–30 GHz but goes up over 30–32 GHz. However, the changes of α have little influence on IBW except few shifts of the resonant frequencies at 26.5 and 30.5 GHz. This is because α has an influence on the strength of the horizontal current.

With the increase of k, the $|S_{11}|$ over 28–31.5 GHz has got up and the IBW have narrowed consequently, as shown in Fig. 4. Besides, the resonant frequencies at 26.5 and 30.5 GHz have shifted toward higher frequencies. Compared to changes of $|S_{11}|$, the effects it brings on AR performance are dramatical. When k is equal to 1, a relative low AR curve is achieved during 24–30 GHz, but the ARBW is the narrowest one, which is the opposite of that k equals to 0.92. For a compromise, 0.96 is taken as the optimal value of k.

When L_{t0} increases, the total helix is lengthened. Thus, the resonant frequencies are shifted down, as shown in Fig. 5. When L_{t0} is 3.74 mm, the AR performance is deteriorated a lot over 30–32 GHz. When L_{t0} is 3.34 or 3.54 mm, the distinction on AR performance is little.

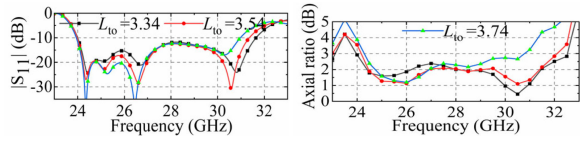

Fig. 5. Simulated performances of $|S_{11}|$ and AR versus L_{t0}.

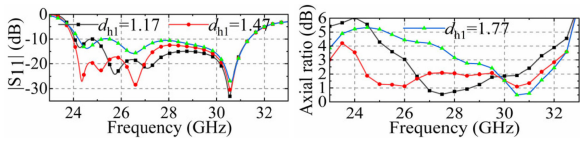

Fig. 6. Simulated performances of $|S_{11}|$ and AR versus d_{h1}.

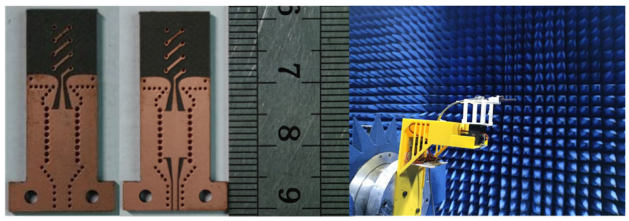

Fig. 7. Pictures of the proposed antenna and measured in microwave anechoic chamber.

As mentioned in antenna operating principle section, the inner ground edges also have made a great contribution on CP radiation as well as IBW. It also can be verified in Fig. 6. With small changes of d_{h1}, the AR performance has been significantly worsened. For the $|S_{11}|$ curve, we can find that the variations of d_{h1} have more impact on lower frequency band (24–29 GHz) but little on higher band (29–32 GHz). When d_{h1} is 1.47 mm, there exist several resonant points around 25 GHz achieving better impedance matching. In this case, 1.47 mm is selected as the optimal value of d_{h1} in terms of fine AR and $|S_{11}|$ simultaneously.

C. Design Procedure

In order to further illustrate the key points of the antenna, a design procedure is given.

1) First, the working bandwidth is set to 24.25–29.5 GHz by turning the parameters related to helix including the length L_t, width W_t, and rotation angle α. Then, determine the number of helical strips by simulation.
2) For broadening the IBW and ARBW, as shown in Fig. 6, the tapered ground with vertical side- and back-wall is designed.
3) Design the transform part between the SIW and helix strips.
4) Design GCPW and SIW-to-GCPW transition for measurement.

III. EXPERIMENTAL RESULTS

A prototype of the antenna has been fabricated and then measured, as shown in Fig. 7. The S-parameter measurement has been finished with an Agilent Network Analyzer AV3672D and the radiation pattern has been measured in a microwave anechoic

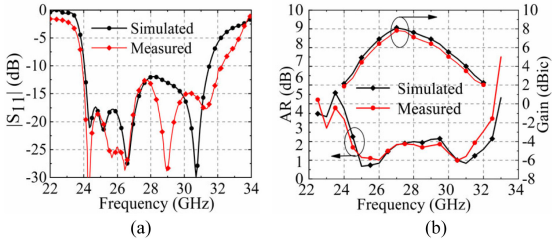

Fig. 8. Simulated and measured (a) $|S_{11}|$; (b) AR and gain.

TABLE II
COMPARISON BETWEEN THE PROPOSED ANTENNA AND THE PREVIOUS DESIGNS

Ref.	Ant. Type	Fre. (GHz)	Ava. (%)	Str.	Feeding network	Size (λ_0)	Gain (dBi)
[4]	Cavity	28	4.6, CP	Pla.	Coa-line	2.0×2.0×0.14	16
[5]	Horn	25	5.9, CP	Pla.	MSL	7.6×4.1×0.12	8.5
[7]	Com.	32	41, CP	Pla.	Waveguide	>0.8×2.9×0.5	12.9
[9]	Helix	10	34, CP	Pla.	Coa-line	1.7×1.6×0.11	8
[10]	Helix	1.7	51, CP	3D.	Coa-line	0.91×0.91×0.98	10.5
[14]	Helix	27	19, CP	Pla.	Dif-fed	/×/×0.14	6.7
[16]	Helix	58	26, LP	Pla.	Coa-line	3.0×1.4×0.07	6.3
This work	Helix	28	29, CP	Pla.	SIW	2.8×1.0×0.14	7.8

Abbreviations: Ref. = Reference, Ant. = Antenna, Fre. = Frequency, Ava. = Available-bandwidth, Pla. = Planar-structure. 3-D = 3D-structure Com. = Complementary antenna. Coa-line = Coaxial line, Dif-fed = Differentially fed.

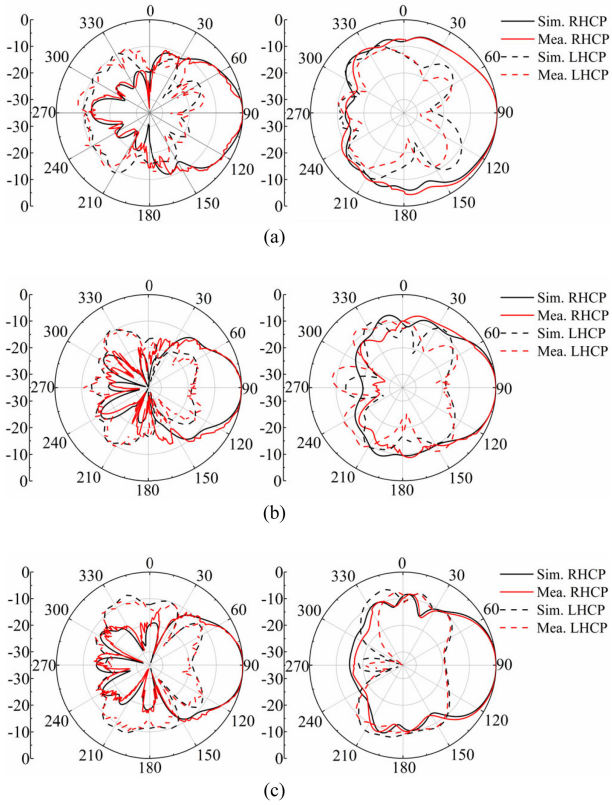

Fig. 9. Simulated and measured radiation patterns. (a) 26 GHz; (b) 28 GHz; (c) 30 GHz. The left column is for *xoy* plane, and the right column is for *yoz* plane.

chamber as well as realized gain and axial ratio. From Fig. 8(a), the measured IBW is 29.3% ranging from 23.8 to 32 GHz, which is about 0.5 GHz wider than the simulated one. The measured resonant frequency at 29 GHz is 1.5 GHz lower than that of the simulated one which can be attributed to the inaccurate of the dielectric constant of the substrate and fabrication tolerances. The measured 3 dB ARBW is 30.4% covering the band from 24 to 32.5 GHz, as shown in Fig. 8(b) and the ARs during 24.5–32 GHz are lower than 2.3 dB. The ARs are slightly higher than the simulated result from 24.5 to 26.5 GHz, which can be attributed to measurement errors. The measured gain is 0.2 dB lower than the simulated one which may be due to the losses of the substrate and misalignments in measurement. Moreover, the antenna again is positively correlated to the substrate length. Therefore, the antenna gain can be adjustable by applying different lengths of the substrate [7]. In a word, the measured and simulated results are in consistent well.

The normalized simulated and measured radiation patterns at 26, 28, and 30 GHz in the *xoy* and *yoz* plane are depicted in Fig. 9, which are in agreement well with each other. As expected, symmetric unidirectional endfire radiation patterns are achieved due to the symmetric structure and SIW-fed scheme. However, for low profile and planar structure, a small ground with vertical vias is utilized, which results in high backlobe levels and leads to a compromise on front-to-back ratio (FTBR). As a result, the measured FTBR is around 10 dB at 26 GHz. But there are some improvements of FTBRs in higher frequencies which show around 20 and 15 dB at 28 and 30 GHz, respectively. Furthermore, the cross-polarization levels at the vertex direction during the whole operating bandwidth are around −20 dB, which indicates good CP performance is achieved.

Table II makes a detailed comparison between our design and the previous in terms of bandwidths, profile heights, feeding structures, and so on. Compared with the 3-D structure helical antenna [10], the planar ones [14], [16] had lower gains due to the smaller ground planes. Antenna [14] needed two ports for differential feeding scheme, which increased the difficulty for excitation. In [9] and [16], they needed extra spaces for coaxial cables and suffered from asymmetric and degraded radiation patterns. In [4] and [5], their ARBWs were too narrow, which limited their practical broadband applications. Although antenna [16] achieved an extreme low profile height, it only radiated linearly polarized wave. Due to the three-layer dielectric rod, antennas [7] suffered from thick profile and bulky size. In addition, our antenna caters to the demands of MMW circuitry, which requires broadband, compact structure, easy fabrication, and low cost.

IV. CONCLUSION

A wideband compact double-helix antenna with circular polarization has been studied in this letter. Through fabrication and test, good agreement is achieved in terms of IBW of 29.3%, ARBW of 30.4% and an overlapped bandwidth of 28.6%. It has the maximum measured gain of 7.8 dBic at the endfire direction. With simple structure, light weight, low cost, and easy fabrication, the antenna is one of the most promising candidates for MMW applications.

REFERENCES

[1] D. J. Bisharat, S. Liao, and Q. Xue, "High gain and low cost differentially fed circularly polarized planar aperture antenna for broadband millimeter-wave applications," *IEEE Trans. Antennas Propag.*, vol. 64, no. 1, pp. 33–42, Jan. 2016.

[2] J. Zhu, S. Liao, Y. Yang, S. Li, and Q. Xue, "60 GHz dual-circularly polarized planar aperture antenna and array," *IEEE Trans. Antennas Propag.*, vol. 66, no. 2, pp. 1014–1019, Feb. 2018.

[3] Y. Li, Z. N. Chen, X. Qing, Z. Zhang, J. Xu, and Z. Feng, "Axial ratio bandwidth enhancement of 60-GHz substrate integrated waveguide-fed circularly polarized LTCC antenna array," *IEEE Trans. Antennas Propag.*, vol. 60, no. 10, pp. 4619–4626, Oct. 2012.

[4] M. Asaadi and A. Sebak, "High-gain low-profile circularly polarized slotted SIW cavity antenna for MMW applications," *IEEE Antennas Wireless Propag. Lett.*, vol. 16, pp. 752–755, 2017.

[5] Y. Yin, B. Zarghooni, and K. Wu, "Single-layered circularly polarized substrate-integrated waveguide horn antenna array," *IEEE Trans. Antennas Propag.*, vol. 65, no. 11, pp. 6161–6166, Nov. 2017.

[6] S. S. Hesari and J. Bornemann, "Wideband circularly polarized substrate integrated waveguide endfire antenna system with high gain," *IEEE Antennas Wireless Propag. Lett.*, vol. 16, pp. 2262–2265, 2017.

[7] J. Wang *et al.*, "Millimeter-wave wideband circularly polarized planar complementary source antenna with endfire radiation," *IEEE Trans. Antennas Propag.*, vol. 66, no. 7, pp. 3317–3326, Jul. 2018.

[8] F. Y. Xia, Y. J. Cheng, Y. F. Wu, and Y. Fan, "V-band wideband circularly polarized endfire multibeam antenna with wide beam coverage," *IEEE Antennas Wireless Propag. Lett.*, vol. 18, no. 8, pp. 1616–1620, Aug. 2019.

[9] Z. Chen and Z. Shen, "Planar helical antenna of circular polarization," *IEEE Trans. Antennas Propag.*, vol. 63, no. 10, pp. 4315–4323, Oct. 2015.

[10] Z. Ren, S. Qi, Z. Hu, Z. Shen, and W. Wu, "Wideband water helical antenna of circular polarization," *IEEE Trans. Antennas Propag.*, vol. 67, no. 11, pp. 6770–6777, Nov. 2019.

[11] M. F. Farooqui and A. Shamim, "3-D inkjet-printed helical antenna with integrated lens," *IEEE Antennas Wireless Propag. Lett.*, vol. 16, pp. 800–803, 2017.

[12] H. Nakano, H. Takeda, T. Honma, H. Mimaki, and J. Yamauchi, "Extremely low-profile helix radiating a circularly polarized wave," *IEEE Trans. Antennas Propag.*, vol. 39, no. 6, pp. 754–757, Jun. 1991.

[13] X. Tang, Y. He, and B. Feng, "Design of a wideband circularly polarized strip-helical antenna with a parasitic patch," *IEEE Access*, vol. 4, pp. 7728–7735, 2016.

[14] J. Yang, G. Jin, Y. Xu, and S. Liao, "A planar differential dual helix antenna for 5G millimeter-wave applications," in *Proc. IEEE MTT-S Int. Wireless Symp.*, 2020, pp. 1–3.

[15] S. H. Zainud-Deen, H. A. E. -A. Malhat, N. A. A. S. El-Shalaby, and S. M. Gaber, "Circular polarization bandwidth reconfigurable high gain planar plasma helical antenna," *IEEE Plasma Sci .*, vol. 47, no. 9, pp. 4274–4280, Sep. 2019.

[16] A. H. Naqvi, J. Park, C. Baek, and S. Lim, "V-band end-fire radiating planar micromachined helical antenna using through-glass silicon via (TGSV) technology," *IEEE Access*, vol. 7, pp. 87907–87915, 2019.

[17] A. H. Naqvi, J. H. Park, C. Baek, and S. Lim, "V-band planar helical antenna using TGSV technology," in *Proc. Int. Symp. Antennas Propag.*, 2018, pp. 1–2.

[18] C. A. Balanis, *Antenna Theory: Analysis and Design*, 3rd ed. Hoboken, NJ, USA: Wiley, 2005.

[19] I. Syrytsin, S. Zhang, and G. F. Pedersen, "Circularly polarized planar helix phased antenna array for 5G mobile terminals," in *Proc. Int. Conf. Electromagn. Adv. Appl.*, 2017, pp. 1105–1108.

[20] G. Shin, M. Kong, S. Lee, S. Kim, and I. Yoon, "Gain characteristic maintained, miniaturized LPDA antenna using partially applied folded planar helix dipoles," *IEEE Access*, vol. 6, pp. 25874–25880, 2018.